

Characterization of swelling behavior of carbon nano-filler modified polydimethylsiloxane composites

Journal of Elastomers & Plastics

2021, Vol. 53(8) 955–974

© The Author(s) 2021



Article reuse guidelines:

sagepub.com/journals-permissions

DOI: 10.1177/00952443211006156

journals.sagepub.com/home/jep**Bo Yang, Balakrishnan Nagarajan and Pierre Mertiny**^{ID}

Abstract

Polymers may absorb fluids from their surroundings via the natural phenomenon of swelling. Dimensional changes due to swelling can affect the function of polymer components, such as in the case of seals, microfluidic components and electromechanical sensors. An understanding of the swelling behavior of polymers and means for controlling it can improve the design of polymer components, for example, for the previously mentioned applications. Carbon-based fillers have risen in popularity to be used for the property enhancement of resulting polymer composites. The present investigation focuses on the effects of three carbon-based nano-fillers (graphene nano-platelets, carbon black, and graphene nano-scrolls) on the dimensional changes of polydimethylsiloxane composites due to swelling when immersed in certain organic solvents. For this study, a facile and expedient methodology comprised of optical measurements in conjunction with digital image analysis was developed as the primary experimental technique to quantify swelling dimensional changes of the prepared composites. Other experimental techniques assessed polymer cross-linking densities and elastic mechanical properties of the various materials. The study revealed that the addition of certain carbon-based nano-fillers increased the overall swelling of the composites. The extent of swelling further depended on the organic solvent in which the composites were immersed in. Experimental findings are contrasted with published models for swelling prediction, and the role of filler morphology on swelling behavior is discussed.

Keywords

Polydimethylsiloxane, PDMS, carbon nano-filler composites, swelling behavior, elastic modulus, cross-linking density

Advanced Composite Materials Engineering Group, Department of Mechanical Engineering, University of Alberta, Edmonton, Canada

Corresponding author:

Pierre Mertiny, Advanced Composite Materials Engineering Group, Department of Mechanical Engineering, University of Alberta, 9211-116 Street NW, Edmonton, AB T6G 1H9, Canada.

Email: pmertiny@ualberta.ca

Introduction

Multifunctional polymer composites are polymers with micro or nano-sized additives to expand the functionality of traditional polymers. Additives/fillers with nano-scale dimensions have significant surface area to volume ratios and may result in drastically changed material properties compared to the plain polymers. For example, adding electrically conductive fillers may enable quantum effects inducing electrical conductivity to an insulator polymer, realizing conductive paints and new methods for electromagnetic shielding.¹⁻⁴ The addition of magnetic fillers can produce magnetic polymers for novel applications such as motors, generators and magnetic sensors.⁵ In addition to imparting non-inherent properties to polymers like electrical conductivity and magnetic polarity, nano-fillers may also be used to create polymer composites with enhanced mechanical properties.

Polymers tend to absorb fluids to a certain extent. In general, this phenomenon is caused by intermolecular forces between the solid and fluid phases. Three principle intermolecular forces, namely London dispersion, dipole-dipole interactions, and hydrogen bonding, exist in all materials but vary in terms of their magnitude.^{6,7} The combined value of the three forces defines the magnitude of the total intermolecular forces. When the magnitude and type of intermolecular forces between the two phases are similar, the attraction is strong enough to break the phase bonds and induce swelling. Some engineering applications require polymers to be exposed to a fluid environment that may cause swelling. In some cases, the swelling phenomenon will inhibit the application of the polymer. For example, swelling of polymer seals can result in improper sizing between the seal and the gland that may lead to additional internal stress and higher failure rate, especially in dynamic applications.^{8,9} In microfluidic applications, unwanted dimensional changes due to swelling of the polymer can lead to improper function of the device.^{10,11} Conversely, a strong swelling phenomenon can be utilized to create solvent vapor sensors based on polymer coated diaphragms in nanoelectromechanical systems.¹²

One potential method to control swelling while maintaining the advantages inherent to polymer materials is to combine the polymer with one or more type of micro or nano-filler. The addition of nano-fillers was observed to improve properties of hydrogels, which are polymer networks swollen within water. Nano-fillers can expand applicable ranges of pH or temperature while improving mechanical strength and thermal conductivity in hydrogel sensors.¹³

The fundamentals of swelling link to solubility. Typically, solubility is thought of a solid—i.e. the solute—dissolving into a liquid—i.e. the solvent. However, for materials such as cross-linked polymers that cannot be dissolved, solubility is measured by the degree of swelling where ultimately the liquid “dissolves” into the solid. For this phenomenon to occur, the cohesive energy between the solid and liquid phase must be similar. As seen in equation (1), the cohesive energy, E_c , is defined as the heat of vaporization per volume:

$$E_c = \frac{\Delta H_{\text{vap}} - RT}{V_{\text{molar}}}, \quad (1)$$

where ΔH_{vap} is the heat of vaporization, R is the ideal gas constant, T is the temperature, and V_{molar} is the molar volume. Cohesive energy corresponds to vaporization energy as well as relates to solubility because the energy required to break the intermolecular forces for solubility is similar to the energy required to change a liquid to a vapor phase.^{6,7} Cohesive energy for polymers, which ultimately relates to intermolecular forces, can be quantified via a solubility parameter: the Hildebrand solubility parameter and the Hansen parameter. The Hildebrand solubility parameter, which equals to the square root of the cohesive energy density, $\delta_{\text{H}} = E_c^{1/2}$, measures the total magnitude of the intermolecular forces.^{14,15} The Hansen parameter, i.e. the expansion of the Hildebrand parameter, i.e. $\delta_{\text{H}}^2 = \delta_{\text{LD}}^2 + \delta_{\text{DD}}^2 + \delta_{\text{H+}}^2$, measures the distribution of the three primary intermolecular forces of London Dispersion, dipole-dipole interactions, and hydrogen bonding.^{16,17} Hence, swelling occurs when the magnitude of δ_{H} and the intermolecular forces (δ_{LD} , δ_{DD} , $\delta_{\text{H+}}$) between the polymer and the solvent are similar.

While swelling of a polymer composite can be assumed to occur in a binary solid-liquid system, the presence of a solid particulate phase has been shown to affect liquid solubility into the solid matrix phase. Kraus in his pioneering work¹⁸ laid out two basic scenarios of how filler particles affect swelling under the assumption that the particles themselves are not subject to liquid solubility: (i) particles are completely bonded to the matrix and thus restrict swelling, and (ii) particles are completely unbonded causing a fluid-filled “vacuole” to evolve around each particle upon matrix swelling. The latter scenario thus promotes swelling. Kraus presented two fundamental equations¹⁸ for swelling with completely bonded and completely unbonded particles, i.e. equations (2) and (3), respectively.

$$\frac{v_{\text{ro}}}{v_{\text{r}}} = 1 - m \frac{\phi}{1 - \phi}; \quad m = (3c - 1) - 3cv_{\text{ro}}^{1/3} + v_{\text{ro}} \quad (2)$$

$$v_{\text{ro}}^{-1} = \frac{v_{\text{r}}^{-1} - \phi}{1 - \phi} \quad (3)$$

where v_{r} and v_{ro} are the volume fraction of matrix in the swollen composite system and the swollen matrix without filler, respectively; ϕ is the filler volume fraction and c is a material constant. Equation (2) is often referred to as the Kraus equation, which is a widely used model for predicting swelling effects in filler modified polymer composites, especially with spherical fillers.^{18,19} To increase accuracy, and with the rise in popularity of platelet and fibrous micro- and nano-fillers, a modification to the Kraus equation, the Interface Area Function, was proposed to accommodate other filler shapes.²⁰ For increasing filler loading, these models necessarily predict a reduction in swelling, i.e. $v_{\text{ro}}/v_{\text{r}} < 1$; conversely, for the case of unbonded fillers, $v_{\text{ro}}/v_{\text{r}} > 1$. Notably, none of these models is able to take particle aggregates into consideration.

Swelling experiments and characterizations are mostly performed for the steady-state or equilibrium state of the swelling process. Equilibrium in swelling of a polymer network is the balance of elastic polymer network forces to the osmotic pressure exerted on the polymer by the swelling agent.²¹ Swelling of a polymer occurs at the cross-link junctions where each network strand is being stretch and untangled. The force needed to

stretch and untangle these network strands correlates directly to the elastic modulus. Hence, at the equilibrium swelling each network strand is balance by the stretch of the osmotic pressure and the pull of the material elasticity.

Swelling measurements of filler modified polymer composites have frequently been performed to characterize the cross-linking density of the polymer. For example, swelling studies were performed by Araby et al. to evaluate the cross-linking density of graphene nanoplatelet (GNP) reinforced nanocomposites developed to enhance the electrical and thermal properties of styrene-butadiene.^{22,23} Studies on nanocomposites that treat the characterization of swelling as a primary objective are comparatively rare and relate predominately to applications toward hydrogels. GNP combined with polyvinyl alcohol, polyacrylic acid, and polyacrylamide used as hydrogels were studied for their mechanical and thermal properties. Due to the hydrogels function as absorbent of water, swelling in H₂O were extensively characterized.^{24–28} All of the mentioned studies used a gravimetric methodology to characterize the swelling of nanocomposites.

Swelling measurements are generally completed by two methods: Gravimetric and optical. Gravimetric measurements take into account the ratio of mass between the swollen network and solvent to that of the dry extracted solid.^{29–33} By considering the mass, gravimetric measurements utilize the whole sample volume and anisotropy can be taken into consideration. However, the disadvantage of measuring mass is a propensity for inaccuracy. The swollen network is usually measured in an equilibrium state which provides maximum susceptibility for the solvent to evaporate. Hence, when volatile organic solutions are used as the swelling solution, the mass measurements of the swollen network are lower than the actual mass of equilibrium in the swelling solution. Conversely, optical measurements quantify dimensional changes instead of a mass change.³⁴ Optical swelling measurements typically only quantify two dimensions of a sample, and the swelling volume needs to be extrapolated with an isotropy assumption. However, with an optical measurement system, equilibrium swelling can be measured in the swelling solution, and hence, unlike gravimetric measurements, the evaporation of the swelling solution can be avoided during the swelling measurement.

In this research, carbon-based nano-fillers of various morphologies and their effect on swelling of silicone rubber (poly-dimethyl siloxane - PDMS) matrices is explored. Solvents acetone, chloroform, and toluene were selected as the swelling agents for their ability to swell PDMS while not being too aggressive of a solvent based on their Hildebrand parameters.³⁵ This study involved three types of carbon filler morphologies: GNP, carbon black (CB) and graphene nano-scrolls (NS). The latter is a GNP derivative with a fibrous morphology. It was reported that by immersing GNP in isopropanol, the platelets curl or roll into scrolls.^{36–39} NS are one of the least studied carbon-based fillers, arguably due to the greater efficiency of their counterpart of carbon nano-tubes. Hence, limited information is available in the technical literature relating to possible enhancements of mechanical and physical properties and, in the context of the present work, swelling effects in NS modified polymers. The present study provides an opportunity to expand the knowledge in this field. A facile and expedient methodology based on optical measurements combined with digital image analysis was developed and used to quantify swelling dimensional changes of the prepared composites. Through swelling

Table 1. Test matrix for swelling experiments.

Type of carbon filler	GNP		CB
Co-solution in solution mixing	Cyclohexane	Isopropanol	Isopropanol
Filler morphology in bulk nanocomposite	GNP	NS	CB
Filler loadings	0 vol%, 1 vol%, 2 vol%, 3 vol%, 4 vol%		
Swelling agents	Acetone, chloroform, toluene		

experiments, the objective of this study is to explore the effects of the carbon-based nano-fillers on the swelling behavior of PDMS. The polymer cross-linking density and elastic properties of the prepared polymer and its composites were assessed to elucidate the experimental findings. The latter were briefly contrasted with published models for swelling prediction.

Experimental methodology

Materials

For this study, GNP and CB were received from XG Sciences (type: Grade M; Lansing, MI, USA) and Cabot Corporation (type: Vulcan XC72; Boston, MA, USA), respectively. The nominal particle dimensions and volumetric mass density are 6–8 nm, 25 μm (thickness, diameter) and 2.2 g/cm^3 for the graphene nanoplatelets and 50 nm and 1.8 g/cm^3 for the carbon black. Poly-dimethyl siloxane was purchased from Dow Corning (type: Sylgard 184; Auburn, MI, USA). The solvents cyclohexane, toluene, chloroform, acetone and isopropanol with 99.9% purity were purchased from Fisher Scientific (Hampton, NH, USA). Using these materials, different bulk nanocomposites were prepared and experiments were conducted as per the test matrix shown in Table 1.

Safety

Safety precautions were considered and taken into actions during the manufacturing and experimentation in this study. All manufacturing and experimentation were completed with standard lab safety wearables under proper ventilation. In addition, due to the presence of nano-fillers and hazardous solutions used in the in-situ polymerization and optical swelling experimentation, all processes were completed with the user wearing a fitted respiratory mask with organic vapor/particulate filters.

Material dispersion and manufacturing of bulk nanocomposites

Manufacturing the different bulk nanocomposites was accomplished using the following procedure. A mass of 30 g of PDMS part A, weighed with a 1 mg resolution weighing scale (type: AV213 Adventure Pro, OHAUS, Parsippany, NJ, USA), was first placed into a 500 ml beaker. The desired volume fraction of nanoparticle, i.e. 1 vol%, 2 vol%, 3 vol% and 4 vol% with respect the total polymer amount, was calculated according to the recorded PDMS part A weight and placed into the same beaker. Samples without

nanofiller addition were also prepared following the same fabrication process, which are herein denoted as “0 vol%.” Note that a filler loading past 4 vol% increased the viscosity of the resin/filler mixture to a point where the mixture was unprocessable with the given experimental setup. A co-solution of either isopropanol or cyclohexane, weighted at 400% of the resin/filler mixture weight, was then poured into the beaker. The mixture was then stirred with an impeller agitator (type: BDC 2002 Variable-Speed Stirrer, Caframo, Warton, ON, Canada) at 500 rpm for 5 min to achieve a uniform distribution of the tri-phase solution. A tapered ultrasonic tip (type: Q500 Sonicator, QSONICA, Newtown, CT, USA) was immersed in the tri-phase solution. The solution was placed in a refrigerated water cooling bath set at 5°C (NESLAB RTE-17 Digital Plus Refrigerated Bath, Thermo Scientific, Newington, NH, USA) to slow the evaporation of the co-solution and to reduce heat from sonication. The solution was sonicated in the cooling bath for 10 h at 40% of power of 500 W at 20 kHz.

Following sonication, the solution was placed on a heated magnetic stir at 65°C for 24 h to evaporate the co-solution. To ensure all co-solution was evaporated after magnetic stirring, the solution was placed in an in-house made heated vacuum system at 15 kPa and 65°C for 2 h. The weight of the remaining PDMS part A and nano-fillers were weighed to ensure the co-solution was evaporated.

Following the solvent removal process, PDMS part B curing agent was added to the resin/nano-filler mixture at a 1:10 ratio with respect to the part A and mixed with the mechanical stir at 250 rpm for 10 min. The nanocomposite mixture was then degassed with the vacuum system at 15 kPa and room temperature for 15 min to remove any entrained gasses from the nanocomposite mixture. The nanocomposite mixture was then brought up from room temperature to 40°C which decreased the viscosity to ensure proper pouring out of the beaker. The composite mixture was then poured onto a release agent coated (ToolMates Dry Film Lubricant 6075, AERVOE Industries, Gardnerville, NV, USA) granite surface plate (88N85.01, Lee Valley Tools, Edmonton, AB, Canada) that was pre-heated to 100°C. Spacers with a thickness of 1 mm were placed on the granite plate and a second granite plate was pressed on top of the base. The bulk sample was left to rest overnight for 12 h in an oven at 100°C.

The bulk sample was carefully removed from the granite plates as a whole and left at room temperature to cool and reach equilibrium for 24 h. A 1.0 cm stainless steel punch was used in conjunction with a hand press to extract circular testing samples from each bulk sample.

Optical swelling tests

As shown in Figure 1, five sample disks were placed on top of a stainless steel mesh in a glass petri dish. Each sample disk was then secured under a stainless steel ring. By using the mesh and the ring, the sample was ensured to stay stationary during any movement of the petri dish during the experiment while exposing maximum and consistent surface area of the sample disk to the solution. Prior to the submerging of the samples, the digital image scale was calibrated with a 0.1 mm and 0.01 mm microscope calibration slide (Model A36CALM7, OMAX, Gyeonggi-do, South Korea). As shown in Table 1, the

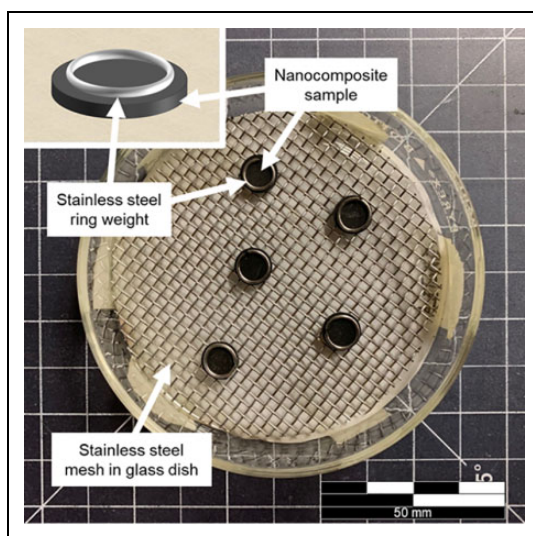


Figure 1. Optical swelling measurement setup with samples submerged in solvent in glass petri dish.

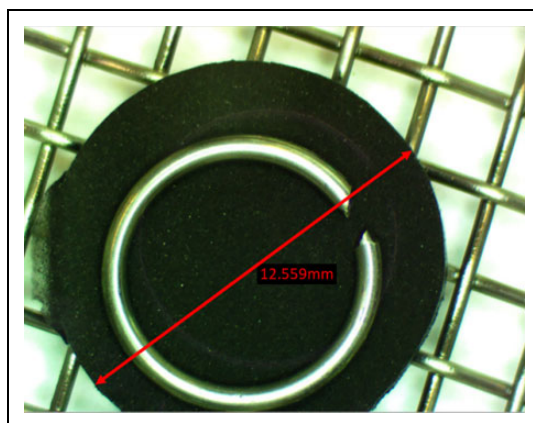


Figure 2. Sample image measurement of 2 vol% GNP/PDMS after being submerged for 8 h.

solvents used as swelling agents were toluene, chloroform, and acetone. The solvent was poured into the petri dish until the top of rings were submerged. Digital images were immediately captured for each sample disks at the 0-h timestamp with the imaging instrument (2X-270X Simal-focal Zoom Stereo Microscope, OMAX). Images were then captured at times of 0.25, 0.5, 1, 2, 4, 8, 12 and 24 h after immersion. As shown by the example in Figure 2, each sample was measured using the ToupView software (version: x64 v3.7.4594, ToupTek, Zhejiang, China).

Cross-linking density characterization

Similar to the work described in refs.^{22,23} cross-linking density characterization was gravimetrically completed. Using the punch and hand press, disk samples were cut from the bulk sample and weighed. Similar to the swelling measurement setup, three disk samples were placed in a petri dish on top of a stainless steel mesh. The disk samples were then submerged in toluene for 24 h. The toluene would swell the polymer sample and flush the polymer network for any oligomers. The nanocomposite disks were then removed from the solution and dried under a fume hood for 24 h, followed by drying under vacuum at 15 kPa and 100°C for 1 h. Mass measurements were taken after the final drying step. The difference in mass between before and after swelling in toluene is the total uncross-linked polymer. Hence, the ratio between the after and before mass is the cross-linking percentage.

Tensile testing

Tensile testing of PDMS and corresponding composites followed the standard ASTM D638-14.⁴⁰ Tensile samples of Type V were produced from the same bulk sample used for the swelling experiments, cut via a water jet. Tensile testing was completed using a universal testing machine (MTS Synergie 300, Eden Prairie, MN, USA). Tests were completed under load control until the break of a sample. Strain was measured using an optical system. For this purpose, each specimen was provided with two high contrasting marks. The optical measurements were completed using an in-house developed software^{41,42} which calculates the strain on a sample by determining the change in distance between the marks. The software utilizes two error functions to determine the positions of the edges of the two marks and thus determines the distance between them. Engineering stress and strain were computed from the recorded load and displacement data, and the modulus of elasticity for the various materials was determined within an initial linear section of the stress-strain curve over approximately 0.10 mm/mm of strain using a linear regression function.

Results and discussion

Swelling characterization of pure PDMS

Dimensional changes in polymer composites due to swelling in organic solvents conducted using optical microscopy are detailed in this section. Note that in the present study, linear swelling ratios rather than volume swelling ratios were measured. The linear swelling ratio is frequently termed q and q_o for a filled and neat matrix material, respectively, and defined as the diameter of a swelled sample, D_s , to the non-swelled condition, D_{us} . Invoking aforementioned isotropy assumption, the corresponding volume swelling ratios are given by $Q = v_r^{-1} = q^3$ and $Q_o = v_{ro}^{-1} = q_o^3$.

Prior to the swelling experiments on carbon nanofiller reinforced nanocomposites, a baseline swelling measurement of un-filled, pure PDMS was conducted. The linear equilibrium swelling ratio for samples immersed in acetone, chloroform, and toluene

Table 2. Linear equilibrium swelling ratios for pure PDMS subjected to solution mixing with different co-solutions.

Co-solution	Swelling agent		
	Acetone	Chloroform	Toluene
—	1.08 ± 0.01	1.30 ± 0.01	1.25 ± 0.01
Cyclohexane	1.08 ± 0.01	1.28 ± 0.01	1.24 ± 0.01
Isopropanol	1.08 ± 0.01	1.30 ± 0.01	1.25 ± 0.01

was found to be 1.08, 1.30, and 1.25, respectively. Lee et al. reported similar swelling ratios for the same swelling agents of correspondingly 1.06, 1.39, and 1.31.³⁴ The repeatability of each sample was high among all samples, that is, all sample points had a standard deviation of approximately 0.01 except for the 0-h time stamp. A higher standard deviation was ascertained at the 0-h time stamp, which is attributed to the transient swelling process. Images for swelling measurements were captured sequentially; therefore, there was an elapsed time of approximately 1 min between the first and fifth sample. For example, the elapsed time, though small, caused an increase of 0.133 in swelling ratio between the first and the fifth sample of pure PDMS submersed in chloroform.

Potential effects of the co-solution used in fabricating the nanocomposites on pure PDMS were also explored. Theoretically, the co-solution only breaks the intermolecular bonds of the PDMS resin. Hence, once a co-solution is fully evaporated, the PDMS resin behaves with no modifications in its monomer structure. As mentioned earlier, pure PDMS samples were made with the same manufacturing process as the nanocomposites without the addition of the nano-fillers i.e. samples were processed with the co-solution, mechanically stirred, and sonicated. The measured linear equilibrium swelling ratios, listed in Table 2, indicate that the used co-solutions only had a negligible effect on the swelling behavior of PDMS when subjected to the different swelling agents.

Transient swelling behavior of carbon filler reinforced nanocomposites

Transient swelling behavior expressed through swelling diameter ratios for GNP, CB and NS composites swollen using the solvents acetone, chloroform and toluene is indicated in Figures 3 to 5, where each data point represents five repeated measurements. The objectives of transient graphs were to confirm the onset of steady-state conditions and to observe any abnormality from the typical transient trend. From the transient graphs it was observed that a steady-state condition was reached around the 4-h mark for all the carbon nanofillers. The overall trend of transient swelling for chloroform and toluene followed expected behavior, i.e. a monotonic and asymptotic increase. However, the trend of transient swelling in acetone exhibited a decrease after an initial peak and minor fluctuation (Figure 3(A) to (C)). The latter seem to indicate small experimental error leading to the observed non-monotonic behavior, yet, a conclusive reasoning remains elusive.

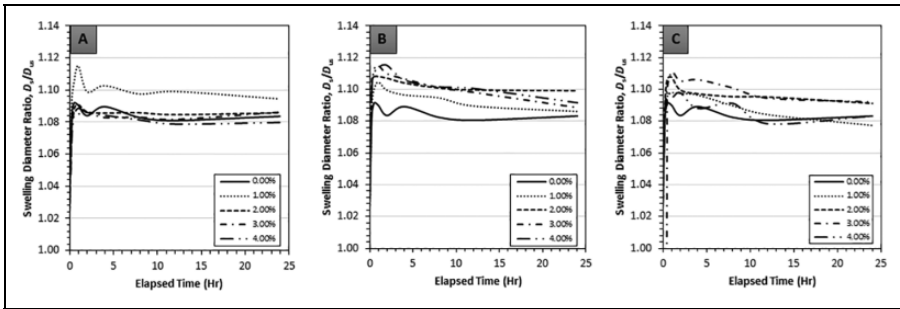


Figure 3. Transient linear swelling ratios of (A) GNP, (B) CB and (C) NS reinforced in PDMS with 0 vol% to 4 vol% filler with acetone as the swelling agent.

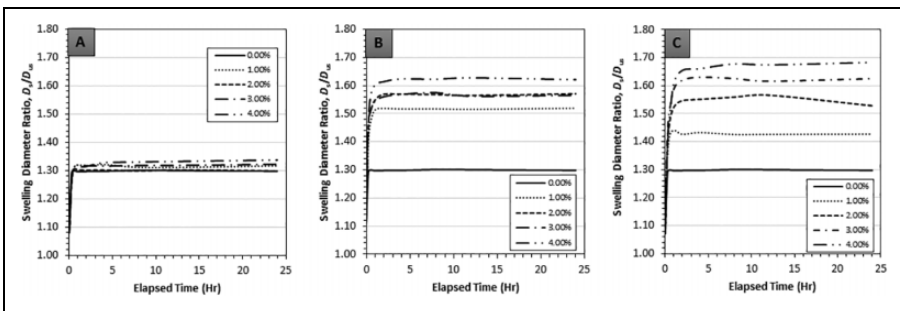


Figure 4. Transient linear swelling ratios of (A) GNP, (B) CB and (C) NS reinforced in PDMS with 0 vol% to 4 vol% filler volume with chloroform as the swelling agent.

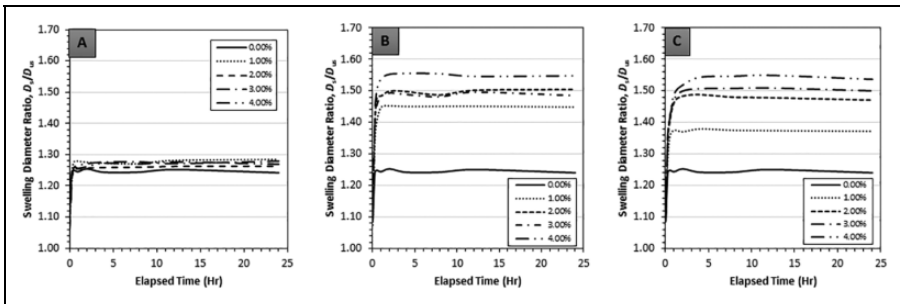


Figure 5. Transient linear swelling ratios of (A) GNP, (B) CB and (C) NS reinforced in PDMS with 0 vol% to 4 vol% filler volume with toluene as the swelling agent.

Equilibrium swelling results of carbon filler reinforced nanocomposites

Linear equilibrium swelling ratios for all PDMS-based samples were computed and are depicted in Figure 8. The data shows an overall strong increase in swelling percentage

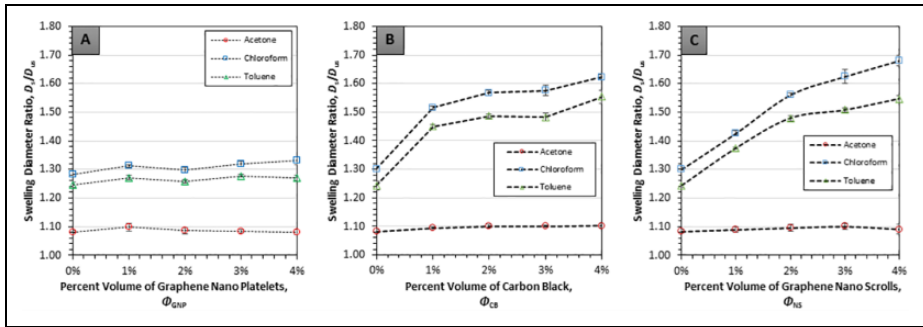


Figure 6. Equilibrium swelling ratio for (A) GNP/PDMS, (B) CB/PDMS and (C) NS/PDMS. Dashed lines are included to guide the eye.

with increasing CB and NS filler volume fraction for nanocomposites swelled with chloroform and toluene. But, for the composites swelled with acetone and those with GNP filler, equilibrium swelling ratios remained close to the unmodified polymer. Referring to Figure 6A, swelling of PDMS composites in acetone was practically independent of filler volume, with the equilibrium swelling ratio remaining at approximately 1.08. Notably, the swelling behavior of the GNP nanocomposites was unlike the trend observed in previous studies with regards to hydrogels^{24–28} where swelling diminished with filler loading. Present findings are more akin to observations described in ref.⁴³ where increased swelling in GNP/PDMS composites over the pure polymer was attributed to a reduction in elastic resistance to swelling stress due to an increase in polymer chain length between cross-links.

For CB/PDMS nanocomposites (Figure 6(B)), the equilibrium swelling ratios in acetone remained approximately between 1.09 and 1.10 and did not change significantly with increasing filler volume fraction. However, CB/PDMS swelled in chloroform and toluene exhibited significant changes, that is, the swelling ratio increased by 25.2% and 23.6% from 0 vol% to 4 vol% CB, respectively. For comparison, corresponding values for GNP/PDMS were only 3.8% in swelling agent chloroform and 2.8% in toluene. It should be mentioned that there is a difference between the percent mass content between GNP ($\rho = 2.2\text{g/cm}^3$) and CB ($\rho = 1.8\text{g/cm}^3$). Nevertheless, by accounting for the density difference at approximately 7% mass content (6.6% mass of GNP and 7.2% mass of CB), the swelling ratio had a similar percent difference of 26% in chloroform and 25% in toluene.

The equilibrium data for NS/PDMS composites (Figure 6(C)) indicates that an increase in filler volume percentage caused an increase of swelling ratio with swelling agents of toluene and chloroform, whereas similar to both GNP/PDMS and CB/PDMS, the swelling of NS/PDMS in acetone remained at ratios between 1.08 and 1.09 with increasing filler volume. With the swelling of NS/PDMS, a monotonic increase appears to be present between the filler volume and the swelling ratio. This trend was not distinctly seen in either the GNP or the CB-based composites. The overall swelling ratio of NS/PDMS increased respectively by 28.9% and 22.8% from 0 vol% to 4 vol% filler

loading in chloroform and toluene. These values are similar to CB/PDMS yet distinctly differed from its parent filler in GNP/PDMS.

To summarize the swelling characterization results, the transient graphs indicate that swelling equilibrium was reached around the 4-h mark, and the morphology of the nano-filler did not appreciably affect the steady-state time. With regards to filler type, the equilibrium results of the three nanocomposites of GNP/PDMS, CB/PDMS and NS/PDMS displayed rather different results with respect to the effect of filler morphology on swelling of PDMS nanocomposite. CB/PDMS and NS/PDMS showed similar significant equilibrium swelling ratios in terms of total increase for the swelling agents of chloroform and toluene but differed somewhat in overall trend and magnitude. In contrast, GNP/PDMS exhibited practically no increase in swelling ratio as filler volume increased. For swelling in acetone, all volume percentages of all three carbon-based filler nanocomposites, as well as the original polymer, exhibited comparable equilibrium swelling.

The Kraus equation and modified Kraus equation mentioned earlier are clearly unable to predict the results from the present experimental study, that is, both equations necessarily predict diminishing swelling volume for increasing filler loading ($v_{ro}/v_r > 1$). The ascendant trend observed in the present experiments ($v_{ro}/v_r < 1$) is compatible with the model for completely unbonded particles according to equation (3). However, following the notion of fluid filling the space around each unbonded particle in the swollen matrix, the corresponding volume $\phi(q_o^3 - 1)$ [18] of solvent is comparatively small. For example, considering PDMS with 4 vol% NS swelled in chloroform, the predicted linear equilibrium swelling ratio is merely 1.31 from 1.30 for pure PDMS compared to the experimentally determined value of 1.68. Consequently, other effects besides the assumptions made by Kraus,¹⁸ i.e. disbonded individual particles, must have led to the more intense swelling behavior observed for the CB and NS fillers.

Cross-linking density characterization

Since a lack of cross-linking can lead to an increase in swelling, the relationship between cross-linking density (or percentage) to swelling ratio as filler percentage increases was explored. Cross-linking density for all the bulk samples was characterized gravimetrically to assess the cure completion of the nanocomposite and possibly correlate the effect of nanofillers to the swelling behavior of the composites. Cross-linking density characterization was also used to confirm that the co-solution had no significant effects on polymer cross-linking, and that the nanofillers were the primary influence. Specifically, it was hypothesized that the co-solution affects the nanocomposite morphology, which ultimately leads to the observed swelling behaviors. As shown in Table 3, the cross-linking percentage of the filled PDMS decreased to some extent as the filler percentage increased with the exception of GNP/PDMS where the decrease was less than 1%.

Figure 7 shows the graphical representation of the relationship between linear equilibrium swelling ratio and cross-linking density with data points left to right corresponding to 4 vol%, 3 vol%, 2 vol%, 1 vol%, and 0 vol% of the different carbon nanofillers.

Table 3. Cross-linking percentage of GNP/PDMS, CB/PDMS and NS/PDMS.

Filler loading	% Cross-linking		
	GNP/PDMS	CB/PDMS	NS/PDMS
0 vol%	95.8%	95.5%	95.5%
1 vol%	95.4%	94.4%	95.2%
2 vol%	95.0%	93.1%	95.2%
3 vol%	95.2%	91.8%	93.1%
4 vol%	95.0%	91.3%	92.0%

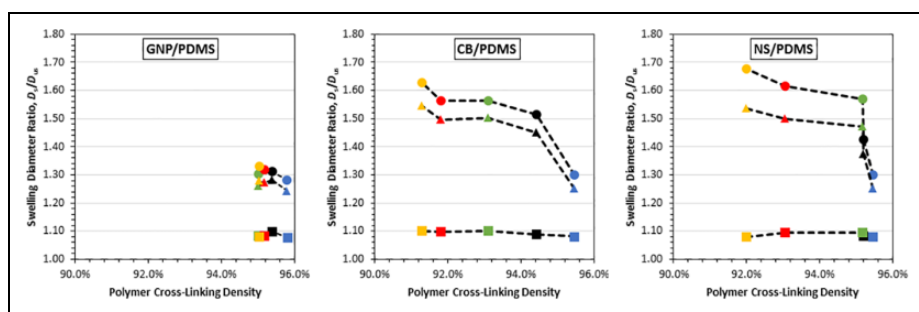


Figure 7. Linear equilibrium swelling ratios of (A) GNP/PDMS, (B) CB/PDMS and (C) NS/PDMS versus cross-linking density. Color of data points corresponds to filler volume percentage: Blue—0 vol%, black—1 vol%, green—2 vol%, red—3 vol%, yellow—4 vol%. The shape of data points corresponds to swelling solution: Circle—chloroform, triangle—toluene and square—acetone. Dashed lines are included to guide the eye.

As observed in Figure 7(A), the GNP/PDMS nanocomposites did not exhibit any appreciable relationship between swelling ratio and cross-linking density as filler loading increased, i.e. all the data points cluster between 95% and 96% cross-linking devoid any strong correlation with swelling ratio. This lack of correlation indicates that the presence of GNP did not appreciably inhibit the cross-linking of PDMS.

In contrast to the GNP filler, CB/PDMS exhibited a noticeably different behavior, as shown in Figure 7(B). A strong rise in swelling diameter ratio can be observed between pure PDMS and 1 vol% CB filler loading. Notably, even the presence of the lowest CB volume fraction in the system swelled the network drastically without strongly compromising cure compared to pure PDMS, i.e. 1 vol% filler loading increased swelling by approximately 20% over pure PDMS in swelling agents of chloroform and toluene. At higher volume percentages, there was a decrease in cross-linking density from values in the upper half of 95% for pure PDMS to as low as 91.3% at 4 vol%. This decrease in cross-linking may have contributed to the increase in swelling but is not seen to be the sole factor.

As shown in Figure 7(C), the relationship between swelling ratio and the cross-linking density for NS/PDMS was observed to be similar to CB/PDMS, i.e. a strong rise in

swelling appeared in chloroform and toluene with the mere presence of 1 vol% NS. However, different from the CB/PDMS where the increase of filler percentage caused a roughly gradual incremental decrease in cross-linking density, a major decrease in cross-linking density in NS/PDMS occurred between 2 vol% to 3 vol% filler. An increase of 26.8% and 21.9% in swelling ratio with swelling agents of chloroform and toluene was observed for a filler increase from 0 vol% to 2 vol%; however, there was a minimal change of cross-linking density. Hence, the initial increase of swelling ratio seems to occur predominantly due to the presence of NS, while the latter increase at higher filler volume may be attributed to both the presence of NS and reduced cross-linking.

The three graphs correlating swelling ratio and cross-linking density show that swelling increases drastically with similar cure completion to that of the plain polymer at the lowest CB and NS filler volume. On the other hand, cross-linking densities for all GNP/PDMS composites were similar to pure PDMS; hence, the observed minor increase in swelling ratio in the swelling agent's chloroform and toluene is likely attributable to the addition of GNP. Overall, the findings derived from the cross-linking density analysis substantiate the initial conclusion that the presence of fillers promoted swelling. The new insight gained from the cross-linking correlation toward the swelling ratio is that at higher percentages of CB and NS, the swelling increase may not have been solely due to the addition of fillers but possibly also due to some lack of cure completion.

Tensile testing

As mentioned earlier, the stretching and untangling of network strands in the swelling of a polymer is directly related to the material's elasticity. Moreover, considering the substantially higher elastic modulus of the carbon filler particles compared to PDMS, and invoking a rule of mixture argument, it stands to reason that filler addition may increase the elastic modulus of the composite over the neat polymer. It should be mentioned that the elastic modulus of PDMS and its composites depends strongly on thermal history.⁴⁴ The same study showed that the addition of GNP may significantly reduce the composite modulus, which was explained with reduced cross-linking of PDMS. In the present study, commencing the analysis with neat PDMS processed without co-solution, the elastic modulus was found to be 2.46 MPa, which falls within the range of values reported by other researchers.^{45,46} Elastic moduli for the various materials processed via solution mixing are listed in Table 4.

Considering the PDMS samples without nanofiller but treated with the different co-solutions, a 14% reduction in modulus can be observed for the samples prepared with isopropanol (CB/PDMS and NS/PDMS) compared to the ones made with cyclohexane (GNP/PDMS).

For the GNP/PDMS nanocomposites, the data reveals that filler addition resulted in a minor decrease in modulus over the neat polymer, with a maximum decrease of 8.5% at 3 vol%. Conversely, the addition of CB caused a significant reduction in elastic modulus. The addition of only 1 vol% CB yielded a modulus reduction to about one-third of the neat PDMS. However, from 1 vol% and 4 vol% CB the modulus decreased to a much lesser extent, i.e. by about 10% with respect to 1 vol%. Similar behavior was observed

Table 4. Tensile modulus of GNP/PDMS, CB/PDMS and NS/PDMS. Numbers in parathesis indicate the standard deviation for tests conducted in triplicate.

Filler loading	Tensile modulus (MPa)		
	GNP/PDMS	CB/PDMS	NS/PDMS
0 vol%	2.71 (0.06)	2.32 (0.05)	2.32 (0.05)
1 vol%	2.49 (0.08)	0.79 (0.03)	1.52 (0.07)
2 vol%	2.52 (0.03)	0.76 (0.02)	1.46 (0.13)
3 vol%	2.48 (0.09)	0.71 (0.07)	1.26 (0.04)
4 vol%	2.59 (0.03)	0.71 (0.04)	1.52 (0.04)

for NS/PDMS where the modulus decreased by a factor of 1.5 between pure PDMS and 1 vol% NS. This substantial decrease was again followed by small changes in modulus between 1 vol% and 4 vol%.

Roy et al. attributed decreasing moduli of CB filled rubber composites to poorly structured CB.⁴⁷ Supposedly, the decrease in modulus observed in the present study stems from increasingly agglomerated CB within the nanocomposites, where agglomerations acted as imperfections inside the material, causing reduced material stiffness. A similar rationale was reported by Jana et al. for silica particles in epoxy.⁴⁸ Even though results were for different filler types, the explanation by Jana et al., i.e. aggregates substantially weakened the material integrity, is considered probable also for present experiments. Consequently, nano-filler aggregation is assumed to be the primary reason for both the increase in swelling ratio and the reduction in mechanical properties. It should be noted at this juncture that decreasing mechanical properties may also be caused by a lack of cross-linking instead of filler agglomeration. However, this notion is rebutted by the data shown in Figure 8. Considering CB/PDMS, a 2.5 fold decrease in modulus from pure PDMS to 1 vol% CB only correlated to approximately a 1% decrease in cross-linking density while the remaining data for 2 vol% to 4 vol% CB shows insignificant modulus reductions with decreasing cross-linking density. Hence, it can be inferred that cross-linking had a negligible effect on modulus in contrast to the presence of the filler and its possible agglomeration. Observations are similar for NS/PDMS which exhibited a large decrease in modulus but only a small reduction in cross-linking density (0.5%) between pure PDMS and 1% NS/PDMS. After the initial strong drop in modulus, the modulus remained approximately constant while cross-linking density was further reduced with increased filler content. This result corroborates the assumption that nano-filler morphology rather than cross-linking density chiefly affected the elastic properties. The present observations give rise to the notion that swelling of the polymer matrix can be tailored by nanofiller addition but requires understanding the complex effects related to nanocomposite morphology including the influence of the co-solution on the filler, the mechanisms controlling the extent of filler dispersion and possible re-agglomeration, the polymer-filler interaction (bonding), and the formation of the polymer network structure.

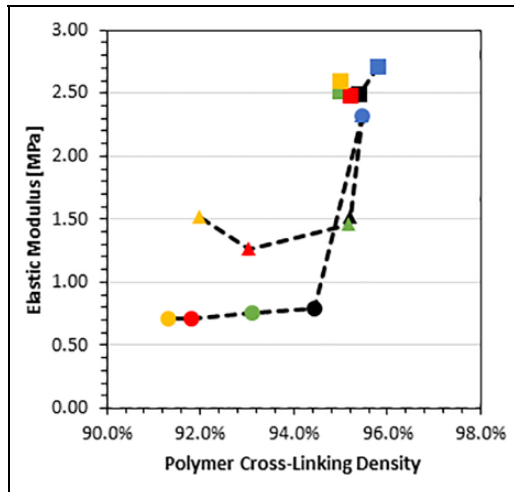


Figure 8. Tensile modulus versus cross-linking density. Color of data points corresponds to filler volume percentage: Blue—0 vol%, black—1 vol%, green—2 vol%, red—3 vol%, yellow—4 vol%. The shape of data points corresponds to filler type: Square—GNP/PDMS, circle—CB/PDMS, and triangle—NS/PDMS. Dashed lines are included to guide the eye.

Conclusions

This study investigated the effects of the carbon-based nano-fillers graphene nano-platelets, carbon black, and graphene nano-scrolls on the swelling of polydimethylsiloxane, with up to 4 vol% filler loading, when immersed in organic solvents acetone, chloroform and toluene. A solution mixing process was employed to fabricate the materials for testing. A facile and expedient methodology comprised of optical measurements in conjunction with digital image analysis was developed and used to quantify transient and equilibrium swelling in terms of linear dimensional changes. In addition to swelling, polymer and composite samples were also assessed for their polymer cross-linking densities and elastic mechanical properties.

The swelling experiments revealed that immersion in acetone caused similar minor dimensional changes, i.e. expansion in the order of 10%, for the pure polymer and all composites irrespective of filler type and loading. In comparison, dimensional changes of the pure polymer in chloroform and toluene was in the order of 20–30%. Testing of the graphene-based composites did not reveal any substantial differences in swelling over the pure polymer. Corresponding elastic moduli and cross-linking densities showed minor reductions upon filler addition. On the other hand, composites with carbon black and graphene nano-scroll fillers, when immersed in chloroform and toluene, exhibited a substantial rise in swelling over the pure polymer. Typically, a great extent of swelling was observed already for the smallest filler loading of 1 vol%, with maximum dimensional changes between 50% and 60% occurring at the highest filler content. Elastic moduli were substantially reduced by about 70% and 30% when the maximum amount of

carbon black and graphene nano-scroll fillers were added, respectively, with a substantial drop occurring already at the lowest filler loading. Cross-linking densities dropped by about 4%.

From the experimental results it was concluded that the solvents chloroform and toluene caused substantial swelling in the studied polymer and composite systems. Moreover, the fillers carbon black and graphene nano-scrolls strongly promoted swelling while also causing a substantial decline in modulus. While reductions in cross-linking density with rising filler content may have contributed to the reduced moduli and the observed ascending trend in swelling, given the considerable extent of properties changes, the presence of the respective fillers is understood to have had further significant effects on the material properties besides cross-linking. Firstly, referring to work by Kraus,¹⁸ filler particles that lack bonding to the matrix are a possible contributor to increased swelling, by facilitating fluid emplacement in the swollen matrix, while also being a probable cause for reduced elastic properties. Secondly, it is reasonable to assume that filler particles agglomerated to some considerable extent in the fabricated composites. The role of filler aggregation, that is, composite morphology, on swelling is an area requiring further study. Furthermore, the study emphasizes the important aspect of filler morphology on composite swelling. Despite having the identical graphene nanoplatelet filler as precursor, the use of different co-solutions in solution mixing led to two material configurations, i.e. graphene composites and nano-scroll composites, which resulted in stark differences in material behavior. In closing, observations made through the present experimental work do not only provide valuable data that can be employed for modeling activities; the study also identifies opportunities for tailoring the swelling behavior of polymer composites, such as the present carbon filler modified polydimethylsiloxane, by means of controlling the filler and composite morphology. In this manner, highly effective materials for novel microfluidic and nanoelectromechanical devices may be realized.


Declaration of conflicting interests

The author(s) declared no potential conflicts of interest with respect to the research, authorship, and/or publication of this article.

Funding

The author(s) disclosed receipt of the following financial support for the research, authorship, and/or publication of this article: This research was funded by the Natural Sciences and Engineering Research Council of Canada (NSERC) through their Discovery Grants program, grant number RGPIN-2016-04650.

ORCID iD

Pierre Mertiny  <https://orcid.org/0000-0001-6117-087X>

References

1. Hussain F, Hojjati M, Okamoto M, et al. Polymer-matrix nanocomposites, processing, manufacturing, and application: an overview. *J Compos Mater* 2006; 40: 1511–1575.
2. Liang J, Wang Y, Huang Y, et al. Electromagnetic interference shielding of graphene/epoxy composites. *Carbon N Y* 2009; 47: 922–925.
3. Chung DDL. Electrical applications of carbon materials. *J Mater Sci* 2004; 39: 2645–2661.
4. Novoselov KS, Fal VI, Colombo L, et al. A roadmap for graphene. *Nature* 2012; 490: 192–200.
5. Filipcsei G, Csetneki I, Szilágyi A, et al. Magnetic field-responsive smart polymer composites. In: Csetneki I, Szilágyi A, Boutevin B, Zrínyi M, Gong B, Filipcsei G, Sanford AE and Boyer C (eds) *Oligomers-polymer composites-molecular imprinting*. Berlin: Springer, 2007, pp. 137–189.
6. Burke J. *Solubility parameters: theory and application*. Vol. 3. AIC Book and Paper Group Annual, 1984, pp. 13–58. <http://cool.conservation-us.org/byauth/burke/solpar> (accessed 24 March 2021).
7. Barton AFM. Solubility parameters. *Chem Rev* 1975; 75: 731–753.
8. How to recognize and avoid the common causes of O-ring failure. <http://www.hydraulicpneumatics.com/200/TechZone/Seals/Article/False/6504/TechZone-Seals> (2000, accessed 24 March 2021).
9. EPM, Inc. *The Seal Man's O-Ring Handbook*. https://projects.iq.harvard.edu/files/epm_oring_handbook.pdf (2004, accessed 24 March 2021).
10. Salimi-Moosavi H, Tang T and Harrison DJ. Electroosmotic pumping of organic solvents and reagents in microfabricated reactor chips. *J Am Chem Soc* 1997; 119: 8716–8717.
11. Kakuta M, Bessoth FG and Manz A. Microfabricated devices for fluid mixing and their application for chemical synthesis. *Chem Rec* 2001; 1: 395–405.
12. Guo H, Lou L, Chen X, et al. PDMS-coated piezoresistive NEMS diaphragm for chloroform vapor detection. *IEEE Electron Device Lett* 2012; 33: 1078–1080.
13. Richter A, Paschew G, Klatt S, et al. Review on hydrogel-based pH sensors and microsensors. *Sensors* 2008; 8: 561–581.
14. Mark JE. *Physical properties of polymers handbook*. Berlin: Springer, 2007.
15. Hildebrand JH and Scott RL. *The solubility of non-electrolytes*. New York, NY: Reinhold Publishing Corporation, 1950.
16. Hildebrand JH and Scott RL. *Regular solutions*. Upper Saddle River, NJ: Prentice-Hall, 1962.
17. Hansen CM. *The three dimensional solubility parameter*. Hørsholm: Danish Tech Copenhagen, 1967.
18. Kraus G. Swelling of filler-reinforced vulcanizates. *J Appl Polym Sci* 1963; 7: 861–871.
19. Anfimova EA, Lykin AS and Anfimov BN. Equilibrium swelling of filled vulcanizates of natural rubber. *Polym Sci USSR* 1982; 24: 455–461.
20. Bhattacharya M and Bhowmick AK. Polymer–filler interaction in nanocomposites: new interface area function to investigate swelling behavior and Young's modulus. *Polymer (Guildf)* 2008; 49: 4808–4818.
21. Rubinstein M and Colby RH. *Polymer physics*. New York, NY: Oxford University Press, 2003.
22. Araby S, Zhang L, Kuan H-C, et al. A novel approach to electrically and thermally conductive elastomers using graphene. *Polymer (Guildf)* 2013; 54: 3663–3670.
23. Araby S, Meng Q, Zhang L, et al. Electrically and thermally conductive elastomer/graphene nanocomposites by solution mixing. *Polymer (Guildf)* 2014; 55: 201–210.

24. Zhang L, Wang Z, Xu C, et al. High strength graphene oxide/polyvinyl alcohol composite hydrogels. *J Mater Chem* 2011; 21: 10399–10406.
25. Shen J, Yan B, Li T, et al. Mechanical, thermal and swelling properties of poly (acrylic acid)–graphene oxide composite hydrogels. *Soft Matter* 2012; 8: 1831–1836.
26. Huang Y, Zeng M, Ren J, et al. Preparation and swelling properties of graphene oxide/poly (acrylic acid-co-acrylamide) super-absorbent hydrogel nanocomposites. *Colloids Surf A Physicochem Eng Asp* 2012; 401: 97–106.
27. Tai Z, Yang J, Qi Y, et al. Synthesis of a graphene oxide–polyacrylic acid nanocomposite hydrogel and its swelling and electroresponsive properties. *RSC Adv* 2013; 3: 12751–12757.
28. Liu R, Liang S, Tang X-Z, et al. Tough and highly stretchable graphene oxide/polyacrylamide nanocomposite hydrogels. *J Mater Chem* 2012; 22: 14160–14167.
29. Favre E. Swelling of crosslinked polydimethylsiloxane networks by pure solvents: influence of temperature. *Eur Polym J* 1996; 32: 1183–1188.
30. Hedden RC, Saxena H and Cohen C. Mechanical properties and swelling behavior of end-linked poly (diethylsiloxane) networks. *Macromolecules* 2000; 33: 8676–8684.
31. Burnside SD and Giannelis EP. Nanostructure and properties of polysiloxane-layered silicate nanocomposites. *J Polym Sci Part B Polym Phys* 2000; 38: 1595–1604.
32. Bandyopadhyay A, De Sarkar M and Bhowmick AK. Polymer–filler interactions in sol–gel derived polymer/silica hybrid nanocomposites. *J Polym Sci Part B Polym Phys* 2005; 43: 2399–2412.
33. Gevers LEM, Vankelecom IFJ and Jacobs PA. Solvent-resistant nanofiltration with filled polydimethylsiloxane (PDMS) membranes. *J Memb Sci* 2006; 278: 199–204.
34. Lee JN, Park C and Whitesides GM. Solvent compatibility of poly (dimethylsiloxane)-based microfluidic devices. *Anal Chem* 2003; 75: 6544–6554.
35. Elif Hamurcu E and Baysal BM. Solubility parameter of a poly (dimethylsiloxane) network. *J Polym Sci Part B Polym Phys* 1994; 32: 591–594.
36. Viculis LM, Mack JJ and Kaner RB. A chemical route to carbon nanoscrolls. (Brevia). *Science (80-)* 2003; 299: 1361–1362.
37. Xie X, Ju L, Feng X, et al. Controlled fabrication of high-quality carbon nanoscrolls from monolayer graphene. *Nano Lett* 2009; 9: 2565–2570.
38. Xia D, Xue Q, Xie J, et al. Fabrication of carbon nanoscrolls from monolayer graphene. *Small* 2010; 6: 2010–2019.
39. Bellido EP and Seminario JM. Molecular dynamics simulations of folding of supported graphene. *J Phys Chem C* 2010; 114: 22472–22477.
40. ASTM D638-14. *Standard test method for tensile properties of plastics*. West Conshohocken, PA: ASTM International, 2014.
41. Raasch J, Ivey M, Aldrich D, et al. Characterization of polyurethane shape memory polymer processed by material extrusion additive manufacturing. *Addit Manuf* 2015; 8: 132–141.
42. Ivey MA. *Towards the development of pseudoductile FRP Rebar*. University of Alberta. <https://era.library.ualberta.ca/items/76df87ed-7ef7-4244-b46b-c2346e1efef6> (2015, accessed 24 March 2021).
43. Berean KJ, Ou JZ, Nour M, et al. Enhanced gas permeation through graphene nanocomposites. *J Phys Chem C* 2015; 119: 13700–13712.
44. Wang X, Shi Z, Meng F, et al. Interfacial interaction-induced temperature-dependent mechanical property of graphene-PDMS nanocomposite. *J Mater Sci* 2020; 55: 1553–1561.

45. Wang Z, Volinsky AA and Gallant ND. Crosslinking effect on polydimethylsiloxane elastic modulus measured by custom-built compression instrument. *J Appl Polym Sci*; 131: 41050.
46. Johnston ID, McCluskey DK, Tan CKL, et al. Mechanical characterization of bulk Sylgard 184 for microfluidics and microengineering. *J Micromech Microeng* 2014; 24: 35017.
47. Roy N, Sengupta R and Bhowmick AK. Modifications of carbon for polymer composites and nanocomposites. *Prog Polym Sci* 2012; 37: 781–819.
48. Jana SC and Jain S. Dispersion of nanofillers in high performance polymers using reactive solvents as processing aids. *Polymer (Guildf)* 2001; 42: 6897–6905.